Nanotechnology **20** (2009) 465602 (5pp) doi:10.1088/0957-4484/20/46/465602

DNA-templated synthesis of Pt nanoparticles on single-walled carbon nanotubes

Lifeng Dong

Department of Physics, Astronomy, and Materials Science, Missouri State University, Springfield, MO 65897, USA

E-mail: LifengDong@MissouriState.edu

Received 17 August 2009, in final form 12 October 2009
Published 21 October 2009
Online at stacks.iop.org/Nano/20/465602

Abstract

A series of electron microscopy characterizations demonstrate that single-stranded deoxyribonucleic acid (ssDNA) can bind to nanotube surfaces and disperse bundled single-walled carbon nanotubes (SWCNTs) into individual tubes. The ssDNA molecules on the nanotube surfaces demonstrate various morphologies, such as aggregated clusters and spiral wrapping around a nanotube with different pitches and spaces, indicating that the morphology of the SWCNT/DNA hybrids is not related solely to the base sequence of the ssDNA or the chirality or the diameter of the nanotubes. In addition to serving as a non-covalent dispersion agent, the ssDNA molecules bonded to the nanotube surface can provide addresses for localizing Pt(II) complexes along the nanotubes. The Pt nanoparticles obtained by a reduction of the Pt^{2+}–DNA adducts are crystals with a size of $\leqslant$1–2 nm. These results expand our understanding of the interactions between ssDNA and SWCNTs and provide an efficient approach for positioning Pt and other metal particles, with uniform sizes and without aggregations, along the nanotube surfaces for applications in direct ethanol/methanol fuel cells and nanoscale electronics.

1. Introduction

Due to their unique structural and electrical properties, carbon nanotubes (CNTs) have been extensively investigated as promising catalyst supports to improve the efficiency of direct ethanol/methanol fuel cells [1–4]. CNTs have a significantly higher electronic conductivity of 10^4 S cm^{-1} and an extremely higher specific surface area of 200–900 m^2 g^{-1} in comparison with the most widely-used Vulcan XC-72R carbon support, which has an electronic conductivity of 4.0 S cm^{-1} and a specific surface area of 237 m^2 g^{-1}. Several approaches, such as electrochemical reduction [5, 6], electroless deposition [7], spontaneous reduction [8, 9], sonochemical technique [10, 11], microwave-heated polyol process [12, 13], and nanoparticle decoration on chemically oxidized nanotube sidewalls [14, 15], have been reported to form CNT-supported platinum (Pt) catalysts. Some remarkable progress has been made in synthesis techniques; however, pioneering breakthroughs have not been made yet in terms of cost-effectiveness catalyst activity, durability, and chemical/electrochemical stability. Major problems hampering the development of CNT-supported Pt catalysts are the lack of reliable approaches for controlling morphology, size, density, and configuration of Pt nanoparticles along carbon nanotubes. The paucity of reports on the synthesis of CNT-supported Pt catalysts, demonstrating controlled properties and structural characterization, is due mostly to the complexity of separating nanotubes, especially single-walled carbon nanotubes (SWCNTs). Nanotubes tend to form bundles due to hydrophobic interactions in aqueous solutions and strong inter-tube *van der Waals* interactions [16–18]. Consequently, most reported attempts have been limited to multi-walled carbon nanotubes (MWCNTs) and bundles of SWCNTs. SWCNTs are expected to have better characteristics as catalyst supports due to their larger surface area and smaller diameters of 0.4–3 nm, in comparison with MWCNTs with diameters of 3–100 nm. Therefore, the aim of this research is to develop an efficient method to synthesize Pt nanoparticles on SWCNTs with controlled properties. The catalytic characteristics of Pt particles are related to their sizes. It is critical to grow Pt nanoparticles with uniform size and lacking aggregation.

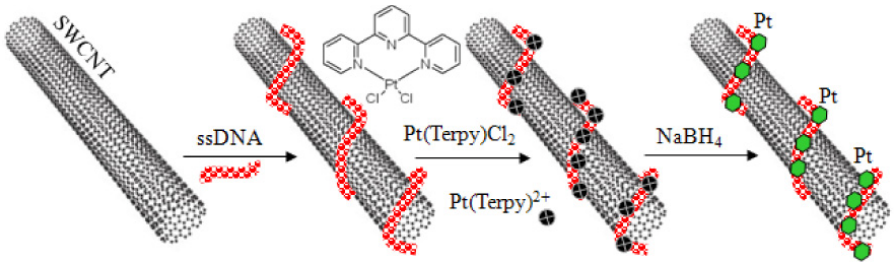

Figure 1. Schematic illustration of controlled synthesis of Pt nanoparticles on a nanotube surface according to ssDNA sites. (This figure is in colour only in the electronic version)

2. Experimental details

2.1. DNA-based dispersion of bundled SWCNTs into individual nanotubes

A desirable approach to producing Pt nanoparticles on SWCNTs must include two processes: the separation of bundled SWCNTs into individual tubes and the synthesis of Pt nanoparticles on the nanotubes. In this study, we used single-stranded deoxyribonucleic acid (ssDNA) molecules to disperse SWCNTs in aqueous solution and as templates for the binding of Pt ions to form Pt nanoparticles along the nanotubes. As illustrated in figure 1, SWCNTs are dispersed first in aqueous solutions in the presence of ssDNA. The SWCNT/DNA complexes are incubated subsequently with Pt ions for a period of time followed by a chemical reduction to form Pt nanoparticles along the SWCNTs. In a typical experiment, 1 mg of nanotube powder (BuckyUSA Company) was suspended in 1 ml ssDNA solution (5′ CCT GAG CCA TGA TCA AAC CTG TGC AGT, 1 mg ml^{-1}, 0.1 M NaCl, Alpha DNA). The suspension was sonicated (Branson Ultrasonic, 130 W) for 60 min. After sonication, the samples were centrifuged (Eppendorf 5415R) for 60 min at 16 000 g. After centrifugation, the supernatant, containing individual SWCNTs, was decanted. The precipitates that contained catalyst particles, bundled nanotubes, and amorphous carbon debris were discarded. The supernatant was dialyzed using cellulose ester membranes with a 100*k* molecular weight cutoff to eliminate free DNA molecules.

2.2. Synthesis of Pt nanoparticles along SWCNTs

For the synthesis of Pt nanoparticles, 100 μl of 0.5 mM Pt(terpy)Cl_2[dichloro(2,2′:6′,2″-terpyridine)platinum(II)] was added to 200 μl of the SWCNT/DNA suspension and incubated at room temperature for 16 h followed by dialysis through cellulose ester membranes to rinse off Pt ions that were not binding to DNA. Finally, 7 μl of 6 mg ml^{-1} of $NaBH_4$ solution was added and incubated at room temperature for 2 h followed by filtering to eliminate free $NaBH_4$ solution.

2.3. Electron microscopy characterization

A series of electron microscopy techniques, including transmission electron microscopy (TEM) and scanning transmission electron microscopy (STEM), were utilized to investigate the morphology, size, and configuration of Pt nanoparticles along the nanotubes. For electron microscopy examinations, several drops of SWCNT/DNA/Pt suspension were transferred onto carbon films supported by the TEM grids. Electron microscopy characterizations were conducted at the National Center for Electron Microscopy (NCEM), located at Lawrence Berkeley National Laboratory, and performed on an FEI F20 UT Tecnai high resolution TEM/STEM at 200 kV and a double-aberration-corrected TEAM 0.5 TEM/STEM at 80 kV [19].

3. Results and discussion

3.1. Morphology of ssDNA/SWCNT hybrids

Since Zheng *et al* [20, 21] successfully used ssDNA molecules to disperse and sort SWCNTs in 2003, a large number of experiments and theoretical simulations have been conducted to study interactions of ssDNA and SWCNTs [22–26]. However, there remains a lack of systematic observations regarding the interfacial structure between the DNA and the nanotube surface. Scanning tunneling microscopy (STM) and atomic force microscopy (AFM) can provide atomic resolution surface and morphology information on DNA/nanotube hybrids, yet it is difficult to use STM and AFM to explore the interfaces. In this study, we used the FEI F20 UT Tecnai TEM/STEM to investigate the morphology and interfacial structures of the hybrids. One nucleotide unit is around 0.34 nm long [27, 28], and the ssDNA used in this study (5′ CCT GAG CCA TGA TCA AAC CTG TGC AGT) is approximately 9 nm long. As demonstrated in figure 2, there are different morphologies for the formed hybrids: some ssDNAs spiral around the nanotubes (indicated by white arrows), and some aggregate around or envelop the nanotubes (indicated by black arrows). This observation suggests that ssDNA molecules with a particular nucleotide sequence can wrap around the same nanotube with different morphologies, such as helices and clusters; therefore, the morphology of the SWCNT/DNA hybrids is not controlled solely by the base sequence of the ssDNA molecules or the diameter and chirality of the nanotubes [29, 30]. The interactions between SWCNTs and ssDNA can be affected by other parameters, such as perturbations from water molecules in solution, CNT structural defects, electrostatic interactions between DNA charges, *van der Waals* and hydrophobic interactions between DNA bases

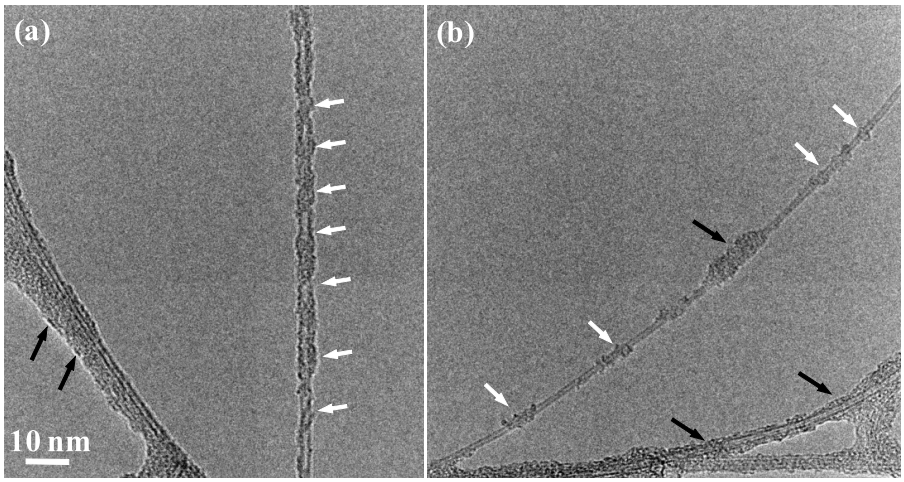

Figure 2. TEM images show that ssDNA molecules effectively disperse bundles of SWCNTs into individual nanotubes. The ssDNA molecules surrounding to the nanotubes display different morphologies; some wrap around the nanotubes with various pitches and spaces (indicated by white arrows), and others aggregate and encapsulate the nanotubes as clusters (indicated by black arrows).

and the CNT, and the sugar and phosphate groups in the DNA backbone. These electron microscopy characterizations are consistent with replica exchange molecular dynamics (REMD) simulations recently reported by Johnson *et al* [31]. They used a large-scale REMD to calculate the free energy landscape of a DNA–CNT hybrid and found energy minima corresponding to six distinct conformations: loop, compact loop, elongated loop, distorted right-hand helix, distorted left-handed helix, and ideal left-handed helix. A non-helical loop structure was the global minimum.

3.2. Z-contrast imaging of the distribution of Pt nanoparticles along SWCNTs

Several groups reported selective synthesis of Pt nanoparticles along DNA molecules:Pt (II) complexes bind primarily to the purine bases, guanine (G) and adenine (A) [32–34]. In this study, we used Pt(terpy)Cl_2, [dichloro (2,2′:6′,2″-terpyridine) platinum(II)], as the Pt(II) complexes. The Cl^- coordinated to Pt^{2+} is labile, whereas the terpyridine (terpy) ligand is non-labile. The $Pt(terpy)^{2+}$ moiety can covalently bind to a purine base, and the Pt^{2+}–DNA adducts can be treated with $NaBH_4$ to reduce Pt^{2+} to Pt^0, thereby forming Pt nanoparticles along nanotubes in accordance with the DNA addresses.

Since Pt has a much higher atomic number Z ($Z = 78$) than those elements in SWCNTs and DNA molecules (phosphorus ($Z = 15$), oxygen ($Z = 8$), nitrogen ($Z = 7$), carbon (C $= 6$) and hydrogen ($Z = 1$)), STEM was employed to investigate the configuration of Pt nanoparticles formed on the SWCNT/DNA hybrids. STEM with a high angle annular dark-field (HAADF) detector is a Z-contrast technique for forming compositional sensitive high resolution images. In this technique, a fine electron beam is scanned across the sample, and the electrons incoherently scattered at high angles are collected by the HAADF detector and used to form an image. As opposed to Bragg-scattered electrons, the high angle scattering is proportional to Z^2, where Z is the atomic number of the species under the probe. The Z-contrast STEM image of the SWCNT/DNA/Pt nanostructures is given in figure 3, in which the heavier atoms appear brighter than the lower Z background structures. Those bright particles are Pt nanoparticles with a size of $\leqslant$1–2 nm. The particles were formed along nanotubes without obvious aggregation. Although we tried to obtain atomic resolutions of the Z-contrast STEM image, the sample was not stable under the electron beam with an acceleration voltage of 200 kV. Subsequently, we attempted to obtain atomic resolution TEM images of the Pt nanoparticles. Similar instability phenomena occurred, and the nanoparticles drifted out of the viewing field during the process of focusing. A lower acceleration

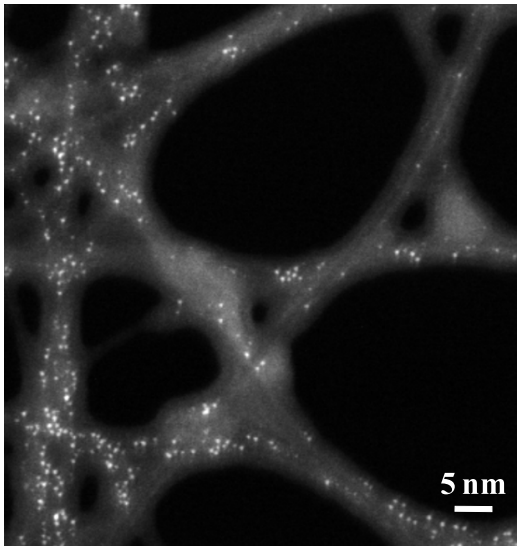

Figure 3. High angle annular dark-field STEM image of SWCNT/DNA/Pt nanostructures demonstrates the distribution of Pt nanoparticles surrounding the nanotubes. Bright particles are Pt nanoparticles with a uniform size of $\leqslant$1–2 nm, and no aggregations exist.

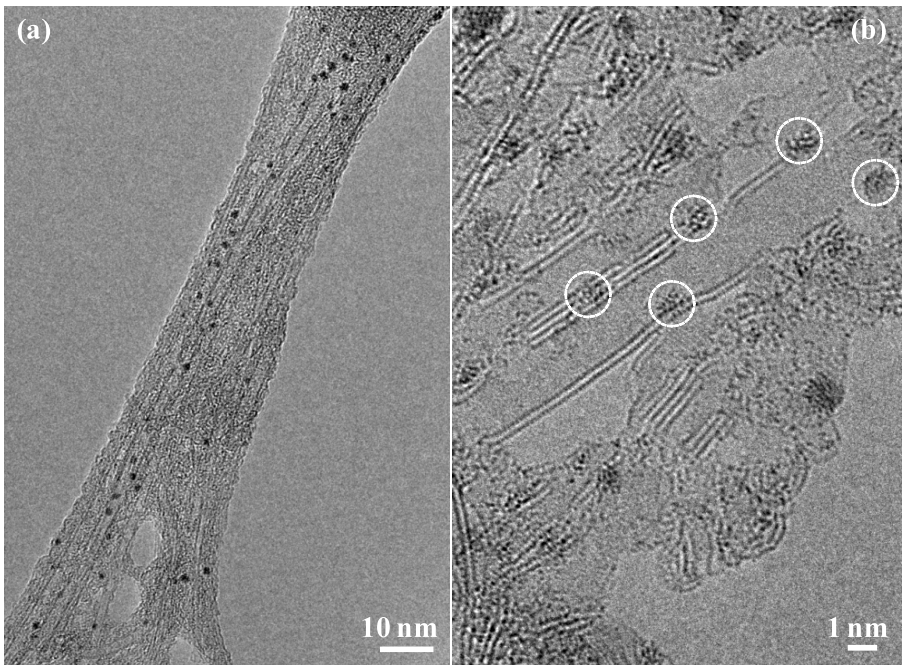

Figure 4. (a) TEM image of SWCNT/DNA/Pt nanostructures shows the configuration of Pt nanoparticles on the nanotubes. While imaging the nanostructures at a higher magnification (b), the nanotubes started to separate from each other, and the configuration of Pt nanoparticles along the nanotubes was revealed. Pt nanoparticles (marked as dashed circles) seem to wrap around the nanotubes in accordance with the ssDNA addresses.

potential must be used to decrease the electron beam damage to the particles and to obtain atomic resolution TEM images. Unfortunately, conventional TEMs demonstrate insufficient resolution at low acceleration voltages. Therefore, we utilized a double-aberration-corrected TEAM 0.5 TEM/STEM. The TEAM 0.5 can achieve sub-angstrom resolution at 80 kV acceleration potential [35].

3.3. Configuration of Pt nanoparticles along SWCNTs

TEM images obtained using the TEAM 0.5 show that Pt nanoparticles seem to selectively form along nanotube surfaces in accordance with the locations of DNA molecules, and no aggregated Pt nanoparticles were observed (figure 4(a)). During nanostructure imaging at a higher magnification (figure 4(b), a higher magnification image of a portion of the nanostructures in figure 4(a)), we exploited the tendency of the focused beam to separate nanotube bundles (figure 4(a)) into smaller fascicles (figure 4(b)) as an in situ dissection method, thereby revealing the configuration of Pt nanoparticles along the nanotubes. Pt nanoparticles (figure 4(b), dashed circles) putatively surround the outer walls of nanotubes, and dark fringes indicate crystal structures of the Pt nanoparticles (figure 4(b)). Both TEM (figures 2 and 4) and STEM (figure 3) characterizations of the SWCNT/DNA hybrids and the SWCNT/DNA/Pt nanostructures verified that the formation of Pt nanoparticles occurs selectively along the surface of SWCNTs following the distribution pattern of DNA molecules. Pt nanoparticles alone or their aggregates were not observed during the TEM/STEM characterizations.

In comparison to the SWCNT/DNA hybrids (figure 2), the SWCNT/DNA/Pt nanostructures (figure 4) were present mainly as bundles during our microscopy examinations. For the SWCNT/DNA hybrid, its dissolution is accomplished via π stacking between the aromatic nucleotides of DNA and the hydrophobic nanotube surface, while the DNA backbone confers water solubility. The binding between nanotubes and DNA is stronger than that among nanotubes, resulting in the dispersion of nanotube bundles into SWCNT/DNA individuals. For the SWCNT/DNA/Pt nanostructures, the binding of $Pt(terpy)Cl_2$ with the nucleotides of DNA, and the reduction of Pt^{2+} to Pt, could reduce the binding affinity between nanotubes and DNA, and *van der Waals* interactions among SWCNT/DNA/Pt nanostructures aggregate them to form bundles.

4. Conclusions

In summary, we have discovered that Pt nanoparticles selectively grow on carbon nanotubes in accordance with ssDNA locations. The ssDNA molecules can not only effectively disperse SWCNT bundles into individual tubes, but also can serve as the address for the formation of Pt nanoparticles along the nanotube surfaces. This finding suggests a method to synthesize other types of carbon-nanotube-supported nanoparticles, such as Pd and Au [36], for applications in fuel cells and nanoscale electronics.

Acknowledgments

This work was partially supported by a Faculty Research Grant and a Summer Faculty Fellowship from Missouri State University and a Visiting Scientist Fellowship from National

Center for Electron Microscopy (NCEM). The author would like to thank Dr Shifeng Hou for providing suggestions on nanoparticle synthesis; Hannah E Gann and Molly Greenwade for their involvement in some of the experiments; and Drs Christian Kisielowski, Thomas Duden, Masashi Watanabe, Zonghoon Lee, and Chengyu Song for their technical support. Acknowledgment is also made to the Donors of the American Chemical Society Petroleum Research Fund (47532-GB10) for partial support of this research. Electron microscopy characterizations were performed at NCEM. The NCEM (Contract No. DE-AC02-05CH11231) and the TEAM project are supported by the Office of Science, Office of Basic Energy Sciences of the US Department of Energy.

References

[1] Planeix J M, Coustel N, Coq B, Brotons V, Sumbhar P S, Dutartre R, Geneste P and Bernier P 1994 *J. Am. Chem. Soc.* **116** 7935
[2] Matsumoto T *et al* 2004 *Cataly. Today* **90** 277
[3] Prabhuram J, Zhao T S, Tang Z K, Chen R and Liang Z X 2006 *J. Phys. Chem.* B **110** 5245
[4] Lee K C, Zhang J J, Wang H J and Wilkinson D P 2006 *J. Appl. Electrochem.* **36** 507
[5] Day T M, Unwin P R, Wilson N R and Macpherson J V 2005 *J. Am. Chem. Soc.* **127** 10639
[6] Quinn B M, Dekker C and Lemay S G 2005 *J. Am. Chem. Soc.* **127** 6146
[7] Qu L T and Dai L M 2005 *J. Am. Chem. Soc.* **127** 10806
[8] Lee Y M, Song H J, Shin H S, Shin H J and Choi H C 2005 *Small* **1** 975
[9] Choi H C, Shim M, Bangsaruntip S and Dai J 2002 *J. Am. Chem. Soc.* **124** 9058
[10] Xing Y C 2004 *J. Phys. Chem.* B **108** 19255
[11] Li L and Xing Y C 2007 *J. Phys. Chem.* C **111** 2803
[12] Li X, Chen W X, Zhao J, Xing W and Xu Z D 2005 *Carbon* **43** 2168
[13] Tian Z Q, Jiang S P, Liang Y M and Shen P K 2006 *J. Phys. Chem.* B **110** 5343
[14] Yu R Q, Chen L W, Liu Q P, Lin J Y, Tan K L, Ng S C, Chan H S O, Xu G Q and Andy Hor T S 1998 *Chem. Mater.* **10** 718
[15] Wang D, Li Z C and Chen L W 2006 *J. Am. Chem. Soc.* **128** 15078
[16] Dong L F, Chirayos V, Bush J, Jiao J, Dubin V M, Chebian R V, Ono Y, Conley J F and Ulrich B D 2005 *J. Phys. Chem.* B **109** 13148
[17] Dong L F, Youkey S, Bush J, Jiao J, Dubin V M and Chebiam R V 2007 *J. Appl. Phys.* **101** 024320
[18] Dong L F, Joseph K L, Witkowski C M and Craig M M 2008 *Nanotechnology* **19** 255702
[19] Girit C *et al* 2009 *Science* **323** 1705
[20] Zheng M, Jagota A, Semke E D, Diner B A, Mclean R S, Lustig S R, Richardson R E and Tassi N G 2003 *Nat. Mater.* **2** 338
[21] Zheng M *et al* 2003 *Science* **302** 1545
[22] Zhao X C and Johnson J K 2007 *J. Am. Chem. Soc.* **129** 10438
[23] Manohar S, Tang T and Jagota A 2007 *J. Phys. Chem.* C **111** 17835
[24] Michalski P J and Mele E J 2008 *Phys. Rev.* B **77** 085429
[25] Johnson R R, Johnson A T C and Klein M L 2008 *Nano Lett.* **8** 69
[26] Martin W, Zhu W S and Krilov G 2008 *J. Phys. Chem.* B **112** 16076
[27] Mandelkern M, Elias J G, Eden D and Crothers D M 1981 *J. Mol. Biol.* **152** 153
[28] Pecora R 1991 *Science* **251** 893
[29] Puller V I and Rotkin S V 2007 *Europhys. Lett.* **77** 27006
[30] Meng S, Wang W L, Maragakis P and Kaxiras E 2007 *Nano Lett.* **7** 2312
[31] Johnson R R, Kohlmeyer A, Johnson A T C and Klein M L 2009 *Nano Lett.* **9** 537
[32] Ford W E, Harnack O, Yasuda A and Wessels J M 2001 *Adv. Mater.* **13** 1793
[33] Mertig M, Ciacchi L C, Seidel R and Pompe W 2002 *Nano Lett.* **2** 841
[34] Stoltenberg R M and Woolley A T 2004 *Biomed. Microdevices* **6** 105
[35] Meyer J C, Kisielowski C, Erni R, Rossell M D, Crommie M F and Zettl A 2008 *Nano Lett.* **8** 3582
[36] Sharma J, Chhabra R, Cheng A, Brownell J, Liu Y and Yan H 2009 *Science* **323** 112